

The Structure of Amine Adducts of Triorganylborexines

Mohamed Yalpani*^a and Roland Boese^b

Max-Planck-Institut für Kohlenforschung^a,
Kaiser-Wilhelm-Platz 1, D-4330 Mülheim an der Ruhr, and
Institut für Anorganische Chemie, Universität Essen^b,
D-4300 Essen 1

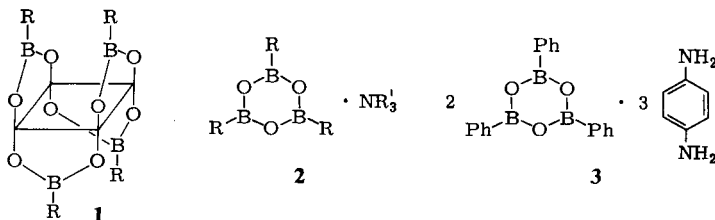
Received February 3, 1983

In a series of donor-acceptor adducts of amines to triorganylborexines (Tables 1, 2) it has been shown by ¹H and ¹¹B NMR spectroscopy that in solution the amine undergoes a temperature dependent fluctuation between the boron atoms of the boroxine ring. In the solid state, as determined by X-ray structural analysis of two selected 3:2 and 1:2 adducts (3 and 6) (boron-nitrogen ratios of 1:1 and 3:1, respectively), only one boron atom of each boroxine ring is involved in adduct formation.

Die Struktur von Amin-Addukten von Triorganylborexinen

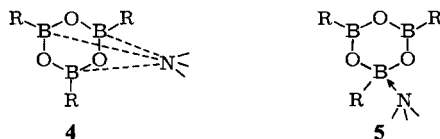
In einer Reihe von Donor-Acceptor-Addukten von Aminen mit Triorganylborexinen (Tabb. 1, 2) wird gezeigt, daß in Lösung die Aminmoleküle zwischen den drei Boratomen des Boroxin-Rings fluktuieren. Im festen Zustand, wie es aus den Röntgenstrukturanalysen von zwei ausgewählten 3:2- und 1:1-Addukten (3 und 6) (mit Bor-Stickstoff-Verhältnissen von 1:1 bzw. 3:1) hervorgeht, ist nur ein Bor-Atom des Boroxin-Rings an der Adduktbildung beteiligt.

Simple and cyclic esters of monoorganylboronic acids act as weak Lewis acids and usually do not form donor-acceptor complexes with amines. We have previously shown that the boron atoms in **1** act as strong acceptors for amines and that adducts with up to four amines per molecule of **1**, i. e., a boron to nitrogen ratio of 1:1, can be formed¹⁾.



This complex forming ability is similar to that of the triorganylborexines which also readily form adducts having the general formula $(\text{RBO})_3 \cdot \text{NR}_3$ (**2**). In all but one of these the amine to boroxine ratio is 1:3 and may formally be regarded as being uniformly bonded to the three boron atoms of the boroxine ring. The only exception is

the 3 : 2 adduct formed by *p*-phenylenediamine and triphenylboroxine ($\text{NH}_2\text{C}_6\text{H}_4\text{NH}_2$)₃ · [(PhBO)₃]₂ (**3**) (boron-nitrogen ratio 1 : 1)²). Although these amine adducts of trialkyl- or triarylboroxines have been known for over fifty years³), their structure and the nature of the bond between the amine and the boroxine ring is still not known with certainty. Thus *Snyder*⁴), from IR data, and more recently *Lutter*⁵), from NMR data (a single ¹¹B signal was observed even at low temperatures), have proposed structure **4** in which the amine is either uniformly bonded to, or in a state of fast exchange between, the three boron atoms. On the other hand *Ritchey*⁶), who has prepared a vast number of these adducts, observed a mysterious "new peak" in the ¹H NMR spectra of the amine adducts of triphenylboroxine and seems to favour structure **5** in which the amine is coordinated to a single boron atom, leaving the other two boron atoms in an sp² environment.



We report here NMR investigations on the structure of a series of such compounds in solution and the determination of the X-ray crystal structure of two selected adducts.

Results and Discussions

A number of amine adducts of trialkyl- and arylboroxines were prepared in the usual manner⁶). Their ¹H and ¹¹B NMR data at room temperature (Tables 1 und 2) clearly show the equivalence of the three B atoms and of the three substituents on the boroxine rings. The range of the ¹¹B chemical shifts shown in Table 1 may be taken as a measure of the degree of interaction of the amine with the boroxine ring and apparently reflect the two factors which influence the adduct strength. A steric factor⁷) makes itself apparent in the lack of a significant shift in the ¹¹B NMR spectra of a 1 : 1 mixture of 2,6-lutidine-triethylboroxine compared to the adducts formed by the less hindered 2,4- and 3,5-lutidines. The second factor affecting the ¹¹B chemical shifts is the Lewis acid and base strength of the acceptor and the donor. Thus the increase of δ¹¹B in the order quinuclidine < Me₃N ≈ 3,5-lutidine < pyridine < quinoxaline, etc. runs essentially parallel to the decreasing values of their p*K*_a's. The amine adducts of triphenylboroxine show a similar trend in their ¹¹B NMR chemical shifts (Table 2). The ¹¹B signals observed for phenylboroxine, however, were in all cases very broad and thus poorly resolved.

Adduct formation and strength is also reflected in the ¹H chemical shifts of the amine as well as of the *B*-alkyl and to a lesser extent of the *B*-aryl moieties. Thus the BEt proton signal which usually appears as a broad singlet at δ = 1.0 resolves into a triplet for the CH₃ group (at a maximum of 0.82 ppm) and a quartet for the boron-bonded CH₂ group (at 0.54 ppm) on increasing the base strength of the amine from quinoxaline to quinuclidine. The change in the chemical shift of the phenyl protons is less significant. However, in all cases only a single resonance pattern was obtained for the A₂B₃ system of the three phenyl ring protons at room temperature.

The high field shift of the amine group signals are also pronounced and similarly reflect the strength of the adducts formed (Table 1). Surprisingly, in the case of the

Table 1. ^{11}B and ^1H NMR chemical shifts of amine adducts of triethylboroxine

Amine	Amine: Boroxine Ratio	$\delta^{11}\text{B}$ (ppm)	$\delta^1\text{H}$ of the amine (ppm)	$\delta^1\text{H}$ of the EtB group
Quinuclidine	—	—	2.82 (dd, 6H); 1.70 (m, 1H); 1.50 (m, 6H)	
Quinuclidine	1:1	23.1	2.93 (dd, 6H); 1.97, 1.70 (m, 6H)	0.83 (t, 9H); 0.54 (q, 6H)
Trimethylamine	1:1	23.9	2.49 (s, 9H)	0.82 (t, 9H); 0.64 (q, 6H)
1,4-Diazabicyclo- [2.2.2]octane	1:2	26.2	3.1 (s, 12H)	0.87 (t, 18H); 0.66 (q, 12H)
Urotropine	1:2	28.3	4.55 (s, 12H)	0.88 (t, 18H); 0.76 (q, 12H)
Pyridine	—	—	8.64 (d, 2H); 7.68 (t, 1H); 7.28 (t, 2H)	
Pyridine	1:1	24.5	8.75 (d, 2H); 8.02 (t, 1H); 7.81 (t, 2H)	0.87 (t, 9H); 0.68 (q, 6H)
3,5-Lutidine	—	—	8.3 (s, 2H); 7.3 (s, 1H); 2.2 (s, 6H)	
3,5-Lutidine	1:1	23.8	8.4 (s, 2H); 7.6 (s, 1H); 2.4 (s, 6H)	0.85 (t, 9H); 0.62 (q, 6H)
2,4-Lutidine	—	—	8.35 (d, 1H); 6.97 (s, 1H); 6.99 (d, 1H); 2.50 (s, 3H); 2.29 (s, 3H)	
2,4-Lutidine	1:1	27	8.82 (d, 1H); 7.06 (s, 1H); 7.10 (d, 1H); 2.80 (s, 3H); 2.31 (s, 3H)	0.83 (t, 9H); 0.76 (q, 6H)
2,6-Lutidine	—	—	7.40 (dd, 1H); 6.80 (d, 2H); 2.47 (s, 6H)	
2,6-Lutidine	1:1	33.5	7.42 (dd, 1H); 6.88 (d, 2H); 2.50 (s, 6H)	0.92 (br.s, 15H)
Quinoxaline	—	—	8.86 (s, 2H); 8.13 (m, 2H); 7.78 (m, 2H)	
Quinoxaline	1:1	33.8	8.84 (s, 2H); 8.18 (m, 2H); 7.78 (m, 2H)	0.98 (br.s, 15H)

Table 2. ^{11}B NMR chemical shifts of amine adducts of triphenylboroxine

Amine	$\delta^{11}\text{B}$ (ppm)
	30.4
Hexamethylenetetraamine	25.1
1,4-Diazabicyclo[2.2.2]octane	22.2
Pyridine	20.5
Quinuclidine*)	19.5
Morpholine	18.4

*) The chloroform solution of the quinuclidine adduct showed at room temp. a relatively sharp signal at $\delta = 5.9$ with a broad shoulder at $\delta = 25.0$. The value given in the Table is for a solution at 50°C . A dioxane solution at room temp. and at 50°C gave a signal at $\delta = 20.0$, the signal narrowing down from 1200 Hz at room temp. to 880 Hz, at half height, at 50°C .

quinuclidine adducts, this shift is projected even to the γ -proton of the base and is comparable in value to that observed for the boron trifluoride adduct of this base ($\delta = 3.07, 2.04, \text{ and } 1.75$, for the $\alpha, \gamma, \text{ and } \beta$ protons, respectively).

While low temperature proton NMR studies conducted by *Ritchey*⁶⁾ apparently showed no temperature effect, *Lutter*⁵⁾ reported a significant broadening of the signals of the BMe groups as well as a shift of the ^{11}B signal of a methylamine-trimethylboroxine adduct to about zero ppm which he attributes to the uniform quaternization of the boron atoms.

We have, however, observed that on cooling a dichloromethane solution of the quinuclidine adduct of triethylboroxine to -20°C a splitting of the ^{11}B signal occurs to give a broad signal at $\delta = 30.9$ and a sharper one at 5.7 (Fig. 1, integration 2:1). The

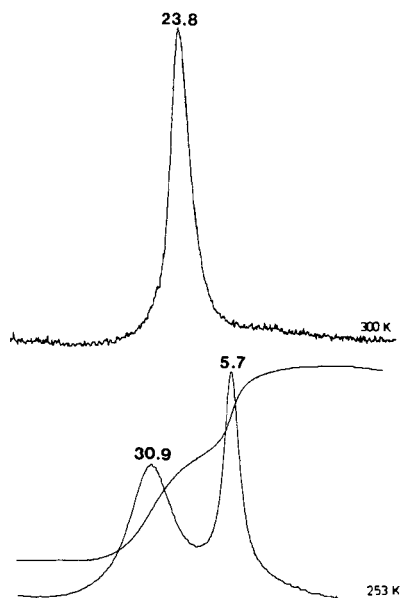


Fig. 1. 64.18 MHz ^{11}B NMR spectrum of $(\text{EtBO})_3 \cdot \text{N}[\text{CH}_2\text{CH}_2]_3\text{CH}$ adduct at 300 and 253 K

first is almost identical to the chemical shift observed for uncomplexed triethylboroxine and thus arise from two sp^2 hybridized boron atoms of the RBO_2 group. The second can be attributed to sp^3 hybridization of the third boron atom of the boroxine ring.

A similar slowing down of the exchange of the amine between the three boron atoms could be observed in the low temperature 1H NMR spectra of several of the adducts studied. Thus the 400 MHz NMR spectrum of a tetrahydrofuran solution of the 1:1 quinuclidine adduct to triphenylboroxine exhibited at room temperature the A_2B_3 spectrum shown in Fig. 2a. Cooling the sample to 230 K resulted in a splitting of the signals to give two A_2B_2C groups as shown in Fig. 2b. The signals at $\delta = 8.13$, 7.41, and 7.23 can be assigned to the *o*, *m*, and *p* protons of the two uncoordinated *B*-phenyl groups. The signals shifted to higher field ($\delta = 7.78$, 7.47, and 7.15) are due to the amine coordinated *B*-phenyl group. In agreement with this assignment the two groups integrate in a 2:1 ratio.

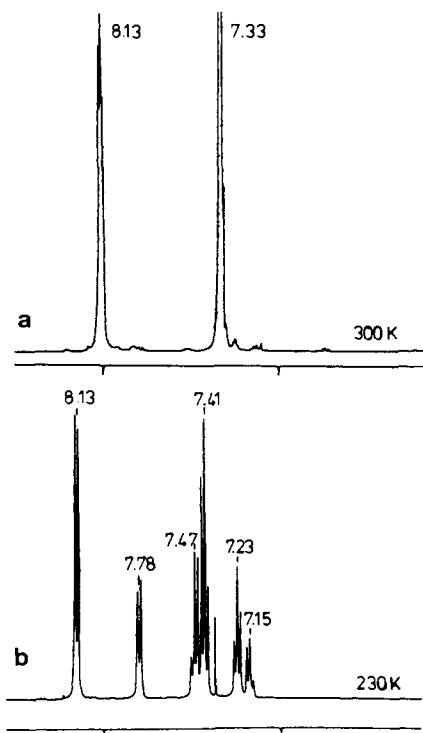


Fig. 2. 400 MHz 1H NMR spectrum of $(PhBO)_3 \cdot$ quinuclidine adduct at 300 and 230 K in CD_2Cl_2

Solid State Structure

The above results clearly show a temperature dependent fluctuation of the amine between the three boron atoms of the boroxine ring in solution and presuppose that in the solid state the amine comes to rest on one of the boron atoms (e.g. 5). To verify this and at the same time to clarify the apparent uniqueness of the 3:2 adduct 3, the solid state structure of the latter was determined by X-ray analysis. The result shown in

Fig. 3 indicates, surprisingly, that only one of the three phenylenediamine molecules is directly involved in the adduct structure. The other two diamine molecules occupy sites at non bonding distances in the crystal lattice and apparently fill the empty space in the lattice structure. Fig. 4 shows the molecules of **3** in the lattice. Other features of the structures are the nearly parallel arrangement of the two boroxine rings above and below the diagonally fixed diamine. The two boroxine rings are conformationally staggered. The phenyl substituents of the tetracoordinated boron atoms are in *anti* position and are bent out of the plane defined by the boroxine ring (maximum deviation from the best plane 0.034 Å) by an angle of 124.5°. The B–N distance of 1.66 Å (cf Table 3) is of the same order as that found in the dipyridine adduct of **1**⁸⁾, in the trimethylamine adduct of boron trichloride⁹⁾ and in the dimeric 2-methyl- Δ^3 -1,2-azaborolines¹⁰⁾. The B–C distances of 1.55 Å for B2–C21 and B3–C31 compared to 1.62 Å for B1–C11 of the *N*-coordinated boron atom indicate a significant electronic overlap of the phenyl substituents with the uncoordinated boron atoms.

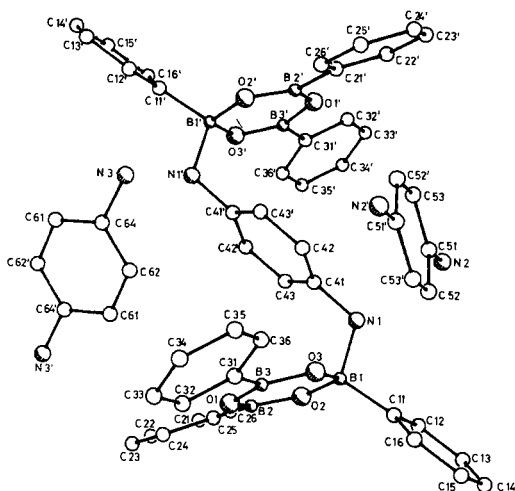


Fig. 3. Molecular Structure of $(\text{PhBO})_3 \cdot p\text{-H}_2\text{NC}_6\text{H}_4\text{NH}_2$ adduct (**3**) with the two *p*-phenylenediamine solvating molecules

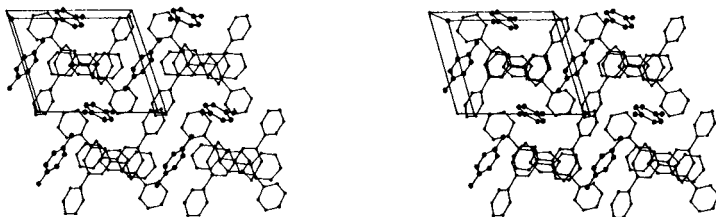


Fig. 4. Packing of molecules of **3** in the crystal

Evident is also some distortion of the boroxine rings. The bond lengths B2–O2 and B3–O3 are significantly shorter than B3–O1 and B2–O1, 1.353 (av) and 1.389 (av),

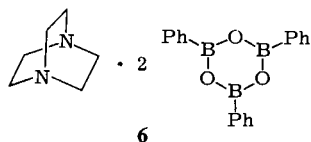
respectively, reflecting a higher π bonding character in these two bonds which presumably reflects the decrease of overlap of the electron pair of O1 with B2 and B3.

Table 3. Bond lengths (Å) and angles (°) for **3**

B(1) - O(2)	1.472(8)	N(3) - C(64)	1.412(10)
B(1) - O(3)	1.444(6)	C(64) - C(61)	1.392(10)
B(1) - N(1)	1.663(8)	C(64) - C(62)	1.388(8)
B(1) - C(11)	1.620(7)	C(62) - C(61')	1.368(10)
B(2) - O(1)	1.389(6)	O(2) - B(1) - N(1)	103.3(4)
B(2) - O(2)	1.350(9)	O(2) - B(1) - O(3)	113.0(5)
B(2) - C(21)	1.554(8)	O(2) - B(1) - C(11)	113.4(4)
		O(3) - B(1) - N(1)	105.7(4)
B(3) - O(1)	1.389(7)	O(3) - B(1) - C(11)	113.9(4)
B(3) - O(3)	1.355(8)	C(11) - B(1) - N(1)	106.3(5)
B(3) - C(31)	1.549(6)	B(1) - O(3) - B(3)	122.9(5)
N(1) - C(41)	1.464(6)		
C(41) - C(42)	1.375(7)	O(3) - B(3) - O(1)	120.4(4)
C(41) - C(43)	1.373(8)	B(3) - O(1) - B(2)	120.4(5)
C(42) - C(43')	1.384(7)	O(1) - B(2) - O(2)	119.9(6)
C(43) - C(42')	1.384(7)	B(2) - O(2) - B(1)	122.9(4)
		B(1) - N(1) - C(41)	115.3(4)
N(2) - C(51)	1.423(5)	O(2) - B(2) - C(21)	121.4(4)
C(51) - C(52)	1.382(7)	O(1) - B(2) - C(21)	118.7(6)
C(51) - C(53)	1.378(7)	O(1) - B(3) - C(31)	118.8(5)
C(53) - C(52')	1.385(6)	O(3) - B(3) - C(31)	120.7(5)

In an attempt to clarify the nature of the interactions, if any, between the two non-bonded *p*-phenylenediamines in the lattice, the adduct was recrystallized from *p*-xylene. The latter, being of approximately the same size and shape, was expected to replace the diamines in the crystallization process. This did not take place. The 3:2 adduct remained intact even after several recrystallizations. We therefore assume that whereas in solution all three diamine molecules remain at bonding distances and undergo a rapid exchange process with the two boroxine rings, in the solid state two of them only contribute to the lattice stability. This is also reflected in the absence of hydrogen bonding as deduced from nearest point of intermolecular contact between the adduct moiety and one of the free diamine molecules (a distance of 2.08 Å between N3 and H - N1').

The necessity for space filling molecules in the crystal lattice of structures like **3** is also observed in the similar 1:2 adduct of 1,4-diazabicyclo[2.2.2]octane with triphenylboroxine N[CH₂CH₂]₃N · [(PhBO)₃]₂ (**6**). In this case the NMR spectra of samples



recrystallized from benzene consistently showed the presence of about three molecules of the solvent. Heating of these crystals led to removal of the solvent molecules but also resulted in the formation of an opaque and amorphous solid. The results of the X-ray analysis of crystalline **6** shown in Fig. 5 clearly indicate the space filling nature of the

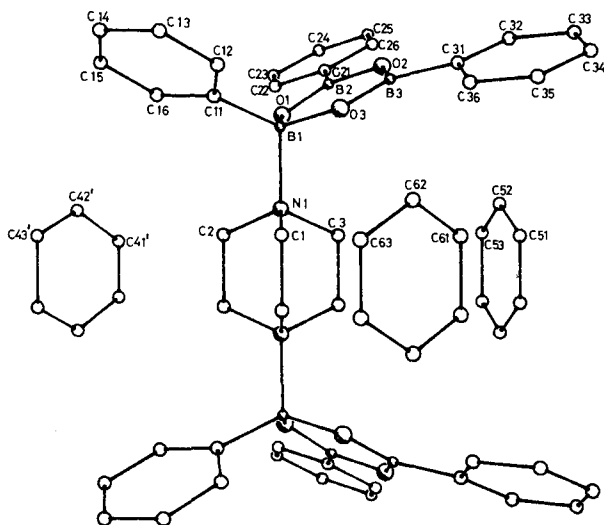


Fig. 5. Molecular structure of $(\text{PhBO})_3 \cdot \text{N}[\text{CH}_2\text{CH}_2]_3\text{N}$ adduct with three solvating benzene molecules

Table 4. Bond lengths (Å) and angles (°) for **6**

B(1) - O(1)	1.450(10)	O(1) - B(1) - O(3)	113.5(6)
B(1) - O(3)	1.463(10)	B(1) - O(3) - B(3)	122.7(6)
B(1) - N(1)	1.714(10)	O(3) - B(3) - O(2)	119.7(6)
B(1) - C(11)	1.633(10)	B(3) - O(2) - B(2)	121.4(6)
		O(2) - B(2) - O(1)	119.2(7)
B(2) - O(1)	1.359(9)	B(2) - O(1) - B(1)	122.9(6)
B(2) - O(2)	1.398(10)	O(3) - B(1) - C(11)	112.7(6)
B(2) - C(21)	1.567(10)	O(1) - B(2) - C(21)	120.9(6)
		O(2) - B(3) - C(31)	120.3(6)
B(3) - O(2)	1.385(9)	O(3) - B(1) - N(1)	102.8(5)
B(3) - O(3)	1.355(9)	C(11)-B(1) - N(1)	110.4(5)
B(3) - C(31)	1.575(9)	B(1) - N(1) - C(1)	111.6(5)
		B(1) - N(1) - C(2)	110.8(5)
N(1) - C(1)	1.504(10)	B(1) - N(1) - C(3)	111.2(5)
N(1) - C(2)	1.496(9)	C(1) - N(1) - C(2)	108.2(5)
N(1) - C(3)	1.509(9)	C(2) - N(1) - C(3)	107.6(5)
		C(3) - N(1) - C(1)	107.3(5)
C(1) - C(1')	1.532(15)	N(1) - C(1) - C(1')	110.9(4)
C(2) - C(2')	1.535(15)	N(1) - C(2) - C(2')	111.0(3)
C(3) - C(3')	1.490(16)	N(1) - C(3) - C(3')	111.7(4)

benzene molecules. The two boroxine rings and their substituents assume an eclipsed conformation above and below the diamine molecule and leave a relatively large empty space which is occupied by the solvent molecules. Fig. 6 shows the molecules of **6** in the lattice. The bond distances and angles (Table 4) are similar to those for adduct **3**. The only major difference is the longer B–N bond distance of 1.71 Å compared to 1.66 Å in **3**. This may arise from the necessity for the two boroxine rings to remain outside the Van der Waal's interaction sphere of the solvent molecules.

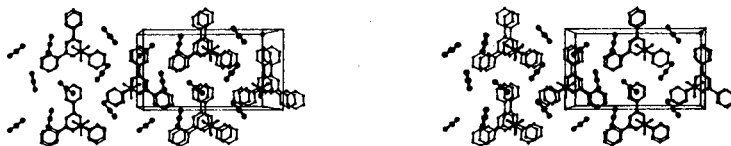


Fig. 6. Packing of molecules of **6** in the crystal

Our results on the nature of the bonding in the amine adducts of the boroxines are thus in agreement with those of the related 1:1 adducts of hexamethylborazine with aluminium tribromide and gallium trichloride in which the donor-acceptor pair have the reversed polarity^{11,12}. One major difference between the two systems is the retention of the planarity of the boroxine ring after coordination to the donor amine in our case whereas the borazine ring is reported to lose its planarity on coordination to the Lewis acid.

We are grateful to Dr. *R. Benn* for measuring the 400 MHz ¹H NMR spectra and M. Y. to *Max-Planck-Gesellschaft* for a fellowship.

Experimental Part

¹H and ¹¹B NMR spectra: Bruker WP 400, WP 80, and Varian XL 100 and 200 instruments. Unless otherwise mentioned, TMS internal standard for ¹H and BF₃ · etherate external standard for ¹¹B.

The amine adducts of triorganylboroxines were obtained from equimolar quantities of the amine and the boroxine in diethyl ether^{4,6}. In those cases where the adducts did not precipitate at room temperature, the solution was cooled to –78 °C and triturated with pentane. Where the adducts were of low stability and did not crystallize, i. e. the 2,4-lutidine adduct, a 1:1 mixture was used directly for NMR measurements.

Structure determination of 3 and 6^{*)}: Crystals of **3** with the dimensions of 0.1 × 0.12 × 0.08 mm and of **6** of 0.2 × 0.1 × 0.28 mm were sealed in a glass capillary and mounted on a Syntex R 3 four-circle diffractometer (Mo-K_α radiation, graphit monochromator). Crystal data can be taken from Table 7. Structure solutions were obtained by direct methods with SHELXTL software¹³ on a NOVA 3/12 (Data General), the structure refinements were performed with SHELXTL

*) Further details and basic data concerning the X-ray analysis may be obtained from Fachinformationszentrum Energie Physik Mathematik, D-7514 Eggenstein-Leopoldshafen (W. Germany), by specifying registry number CSD 50462, author, and source.

Table 5. Atomic coordinates and anisotropic temperature parameter for 3 as $\exp[-2\pi^2(U_{11}h^2a^{*2} + U_{22}k^2b^{*2} + U_{33}l^2c^{*2} + 2U_{12}h^*a^*b^*hk + 2U_{13}h^*la^*c^* = 2U_{23}klb^*c^*)]$ or as $\exp[-8\pi^2 U_{\text{iso}}(\sin \Theta/\lambda)^2]$ (standard deviations in parentheses)

Atom	x	y	z	U_{11}/U_{iso}	U_{22}	U_{33}	U_{23}	U_{13}	U_{12}
B(1)	0.3556(7)	0.3429(5)	0.2840(5)	0.054(4)	0.054(4)	0.059(5)	-0.006(3)	-0.014(4)	-0.018(4)
B(2)	0.5004(7)	0.4611(6)	0.3273(5)	0.056(5)	0.074(5)	0.042(4)	-0.001(3)	-0.008(4)	-0.026(4)
B(3)	0.6232(6)	0.2538(5)	0.2668(5)	0.061(4)	0.039(4)	0.054(4)	0.005(3)	-0.010(3)	-0.019(3)
O(1)	0.6267(3)	0.3590(3)	0.3061(3)	0.055(2)	0.053(2)	0.088(3)	-0.015(2)	-0.015(2)	-0.015(2)
O(2)	0.3704(4)	0.4536(3)	0.3197(3)	0.056(2)	0.045(2)	0.064(3)	-0.012(2)	-0.008(2)	-0.015(2)
O(3)	0.4951(3)	0.2469(3)	0.2536(3)	0.047(2)	0.044(3)	0.074(3)	-0.008(2)	-0.007(2)	-0.014(2)
N(1)	0.3003(4)	0.3990(3)	0.1682(3)	0.048(3)	0.053(3)	0.052(3)	0.003(2)	-0.004(2)	-0.026(2)
N(2)	0.2465(4)	0.2061(4)	0.0634(4)	0.052(3)	0.048(3)	0.111(4)	-0.030(3)	-0.010(3)	-0.010(2)
N(3)	1.0005(5)	0.3863(5)	-0.1776(4)	0.079(4)	0.116(4)	0.109(4)	-0.006(3)	-0.029(3)	-0.023(3)
C(11)	0.2272(4)	0.2901(2)	0.3670(3)	0.053(4)	0.052(4)	0.050(4)	0.001(3)	-0.011(3)	-0.022(3)
C(12)	0.0876(4)	0.3725(2)	0.4055(3)	0.055(4)	0.059(4)	0.073(4)	0.012(3)	-0.002(3)	-0.014(3)
C(13)	-0.0197(4)	0.3276(2)	0.4825(3)	0.059(4)	0.071(4)	0.085(5)	0.007(4)	0.004(4)	-0.020(3)
C(14)	0.0127(4)	0.2004(2)	0.5210(3)	0.078(5)	0.078(5)	0.078(5)	-0.001(4)	0.008(4)	-0.040(4)
C(15)	0.1523(4)	0.1179(2)	0.4825(3)	0.092(5)	0.050(4)	0.081(5)	0.000(3)	0.005(4)	-0.032(4)
C(16)	0.2596(4)	0.1628(2)	0.4055(3)	0.080(4)	0.045(4)	0.065(4)	-0.009(3)	-0.001(3)	-0.025(3)
C(21)	0.5143(4)	0.5844(3)	0.3542(3)	0.057(4)	0.047(4)	0.044(4)	0.002(3)	-0.006(3)	-0.022(3)
C(22)	0.6446(4)	0.5848(3)	0.3757(3)	0.067(5)	0.067(4)	0.069(4)	-0.011(3)	-0.023(3)	-0.022(3)
C(23)	0.6576(4)	0.6960(3)	0.3982(3)	0.073(5)	0.086(5)	0.082(5)	-0.026(4)	-0.017(4)	-0.028(4)
C(24)	0.5403(4)	0.8067(3)	0.3992(3)	0.107(6)	0.060(5)	0.080(5)	-0.018(4)	-0.014(4)	-0.034(4)
C(25)	0.4098(4)	0.8062(3)	0.3778(3)	0.082(5)	0.058(5)	0.094(5)	-0.017(4)	-0.015(4)	-0.021(3)
C(26)	0.3968(4)	0.6951(3)	0.3553(3)	0.066(4)	0.045(4)	0.075(4)	-0.008(3)	-0.007(3)	-0.018(3)
C(31)	0.7690(5)	0.1465(3)	0.2353(3)	0.049(4)	0.049(4)	0.063(4)	0.009(3)	-0.012(3)	-0.020(3)
C(32)	0.8901(5)	0.1383(3)	0.2747(3)	0.051(4)	0.058(4)	0.084(5)	0.014(3)	-0.014(4)	-0.011(3)
C(33)	1.0223(5)	0.0430(3)	0.2451(3)	0.073(5)	0.067(5)	0.108(6)	0.013(4)	-0.017(4)	-0.026(4)
C(34)	1.0333(5)	-0.0441(3)	0.1761(3)	0.067(5)	0.078(5)	0.133(7)	-0.000(5)	0.001(5)	-0.006(4)
C(35)	0.9122(5)	-0.0358(3)	0.1367(3)	0.101(6)	0.070(5)	0.143(7)	-0.040(5)	-0.005(5)	-0.008(5)
C(36)	0.7800(5)	0.0595(3)	0.1663(3)	0.087(5)	0.055(4)	0.109(6)	-0.028(4)	-0.019(4)	-0.021(4)
C(41)	0.4020(5)	0.4519(5)	0.0810(4)	0.049(4)	0.049(4)	0.054(4)	-0.003(3)	-0.007(3)	-0.022(3)
C(42)	0.5062(6)	0.3751(4)	0.0056(4)	0.065(4)	0.032(3)	0.056(4)	0.001(3)	-0.003(3)	-0.021(3)
C(43)	0.3962(6)	0.5755(5)	0.0760(4)	0.054(4)	0.041(4)	0.064(4)	-0.013(3)	0.001(3)	-0.013(3)
C(51)	0.3728(5)	0.1020(3)	0.0313(4)	0.061(4)	0.053(3)	0.068(4)	-0.001(3)	-0.017(3)	-0.025(3)
C(52)	0.4264(6)	0.0076(5)	0.1078(4)	0.064(4)	0.066(4)	0.061(4)	-0.007(3)	-0.005(3)	-0.024(3)
C(53)	0.4495(6)	0.0930(5)	-0.0769(4)	0.076(4)	0.054(4)	0.071(4)	0.005(3)	-0.022(3)	-0.019(3)
C(61)	1.0798(6)	0.5292(6)	-0.1041(5)	0.071(5)	0.094(5)	0.075(5)	0.017(4)	-0.016(4)	-0.022(4)
C(62)	0.9261(6)	0.4127(5)	0.0170(5)	0.069(4)	0.087(5)	0.090(5)	0.028(4)	-0.020(4)	-0.028(4)
C(64)	1.0066(6)	0.4395(6)	-0.0877(5)	0.072(5)	0.073(5)	0.084(5)	0.016(4)	-0.030(4)	-0.016(4)
H(12)	0.0653(4)	0.4601(2)	0.3790(3)	0.131(8)					
H(13)	-0.1158(4)	0.3844(2)	0.5090(3)	0.131(8)					
H(14)	-0.0612(4)	0.1695(2)	0.5740(3)	0.131(8)					
H(15)	0.1746(4)	0.0304(2)	0.5090(3)	0.131(8)					
H(16)	0.3557(4)	0.1061(2)	0.3790(3)	0.131(8)					
H(22)	0.7254(4)	0.5086(3)	0.3749(3)	0.127(9)					
H(23)	0.7474(4)	0.6963(3)	0.4129(3)	0.127(9)					
H(24)	0.5492(4)	0.8831(3)	0.4147(3)	0.127(9)					
H(25)	0.3291(4)	0.8824(3)	0.3785(3)	0.127(9)					
H(26)	0.3070(4)	0.6948(3)	0.3406(3)	0.127(9)					
H(32)	0.8825(5)	0.1982(3)	0.3222(3)	0.169(10)					
H(33)	1.1056(5)	0.0373(3)	0.2722(3)	0.169(10)					
H(34)	1.1243(5)	-0.1096(3)	0.1558(3)	0.169(10)					
H(35)	0.9198(5)	-0.0957(3)	0.0893(3)	0.169(10)					
H(36)	0.6967(5)	0.0652(3)	0.1392(3)	0.169(10)					
H(42)	0.5142(6)	0.2874(4)	0.0114(4)	0.041(7)					
H(43)	0.3237(6)	0.6284(5)	0.1292(4)	0.041(7)					
H(52)	0.3721(6)	0.8094(5)	0.1832(4)	0.073(9)					
H(53)	0.4097(4)	0.1580(5)	-0.1294(4)	0.073(9)					
H(61)	1.1362(6)	0.5385(6)	-0.1782(5)	0.130(15)					
H(62)	0.8745(6)	0.3515(5)	0.0285(5)	0.130(15)					
H(1A)	0.2042(4)	0.4594(3)	0.1839(3)	0.204(18)					
H(1B)	0.2950(4)	0.3284(3)	0.1396(3)	0.204(18)					
H(2A)	0.1535(4)	0.1911(4)	0.0739(4)	0.259(23)					
H(2B)	0.2312(4)	0.2808(4)	0.0963(4)	0.259(23)					
H(3A)	0.9478(5)	0.3453(5)	-0.2042(4)	0.204(18)					
H(3B)	1.1017(5)	0.3642(5)	-0.2179(4)	0.204(18)					

block-cascades least squares. Phenyl groups were refined as rigid groups with a fixed C–C distance of 1.395 Å and C–H distance of 0.96 Å. Hydrogen atoms were refined with a unique isotropic temperature factor for **3** on each individual phenyl group and phenylenediamine group as well as for nitrogen-bonded hydrogens. These positions were calculated and refined on their torsion at C–N bond. Hydrogen atoms bonded to the coordinated nitrogens in **6** were treated as rigid groups as for the phenyl groups but with an isotropic temperature factor for all hydrogens. Methylene hydrogen atoms were located in a difference map, and constrained to the carbon atoms with a distance of 0.98 Å and a unique isotropic temperature factor. The hydrogen atoms at the solvent benzene could not be located in the difference map, being very diffuse because of the disorder of the benzene molecules C(41)–C(44), C(41')–C(43') and C(51)–C(53), C(51')–C(54'). These molecules are rotated by 15° around their centre, situated within the mirror plane at $y = 0.25$. The ratio of the site occupation factors were fixed at 1:1 for C(41)–C(44) and C(41')–C(43'), respectively, and 2:1 for C(51)–C(53) and C(51')–C(54') respectively in order to get approximately the same temperature factors. The final atomic coordinates and anisotropic temperature parameters appear in Tables 5 and 6.

Table 6. Atomic coordinates and anisotropic temperature parameter for **6** as $\exp[-8\pi^2 U_{\text{iso}}(\sin \Theta/\lambda)^2]$ (standard deviations in parentheses)

Atom	x	y	z	U_{iso}	Atom	x	y	z	U_{iso}
B(1)	0.2409(8)	0.1281(3)	0.4455(4)	0.032(2)	C(51)	0.2537(19)	0.2210(8)	0.6985(10)	0.068(5)
B(2)	0.0672(8)	0.0864(3)	0.5025(4)	0.029(2)	C(52)	0.1445(16)	0.1932(6)	0.6852(8)	0.064(5)
B(3)	0.2584(7)	0.0890(3)	0.5608(4)	0.025(2)	C(53)	0.0362(13)	0.2188(6)	0.6742(7)	0.065(4)
O(1)	0.1147(4)	0.1150(2)	0.4500(2)	0.032(1)	C(51')	0.2712(49)	0.2500(0)	0.7033(27)	0.071(17)
O(2)	0.1393(4)	0.0738(2)	0.5584(2)	0.034(1)	C(52')	0.2015(27)	0.2049(11)	0.6973(13)	0.041(8)
O(3)	0.3082(4)	0.1148(2)	0.5070(2)	0.032(1)	C(53')	0.0931(25)	0.2050(10)	0.6785(12)	0.051(7)
N(1)	0.2429(5)	0.1974(2)	0.4451(3)	0.027(2)	C(54')	0.0211(37)	0.2500(0)	0.6688(20)	0.063(12)
C(1)	0.3686(7)	0.2191(3)	0.4439(4)	0.038(2)	C(61)	0.1658(11)	0.2206(5)	0.8943(7)	0.112(4)
C(2)	0.1779(7)	0.2190(3)	0.3844(4)	0.034(2)	C(62)	0.2364(12)	0.1941(5)	0.8249(7)	0.110(4)
C(3)	0.1827(8)	0.2199(3)	0.5077(4)	0.037(2)	C(63)	0.3012(12)	0.2220(5)	0.9933(6)	0.114(5)
C(11)	0.3035(4)	0.1046(2)	0.3765(2)	0.030(2)	H(1)	0.3991(61)	0.2119(28)	0.3980(15)	0.074(11)
C(12)	0.4191(4)	0.0836(2)	0.3806(2)	0.032(2)	H(2)	0.4120(61)	0.2084(26)	0.4850(22)	0.074(11)
C(13)	0.4709(4)	0.0591(2)	0.3239(2)	0.044(2)	H(3)	0.2153(6)	0.2035(28)	0.3438(23)	0.074(11)
C(14)	0.4069(4)	0.0555(2)	0.2631(2)	0.045(2)	H(4)	0.0934(19)	0.2085(28)	0.3866(38)	0.074(11)
C(15)	0.2913(4)	0.0765(2)	0.2590(2)	0.041(2)	H(5)	0.2339(54)	0.2081(29)	0.5454(25)	0.074(11)
C(16)	0.2395(4)	0.1010(2)	0.3157(2)	0.035(2)	H(6)	0.0981(19)	0.2096(29)	0.5096(37)	0.074(11)
C(21)	-0.0680(4)	0.0697(2)	0.5024(2)	0.031(2)	H(12)	0.4631(4)	0.0861(2)	0.4224(2)	0.091(7)
C(22)	-0.1395(4)	0.0813(2)	0.4461(2)	0.038(2)	H(13)	0.5504(4)	0.0447(2)	0.3267(2)	0.091(7)
C(23)	-0.2603(4)	0.0671(2)	0.4463(2)	0.046(2)	H(14)	0.4425(4)	0.0387(2)	0.2240(2)	0.091(7)
C(24)	-0.3095(4)	0.0412(2)	0.5028(2)	0.046(2)	H(15)	0.2473(4)	0.0740(2)	0.2172(2)	0.091(7)
C(25)	-0.2380(4)	0.0296(2)	0.5591(2)	0.037(2)	H(16)	0.1600(4)	0.1154(2)	0.3129(2)	0.091(7)
C(26)	-0.1172(4)	0.0438(2)	0.5589(2)	0.033(2)	H(22)	-0.1056(4)	0.0991(2)	0.4072(2)	0.091(7)
C(31)	0.3342(3)	0.0792(2)	0.6272(2)	0.026(2)	H(23)	-0.3095(4)	0.0751(2)	0.4076(2)	0.091(7)
C(32)	0.2796(3)	0.0572(2)	0.6847(2)	0.033(2)	H(24)	-0.3926(4)	0.0314(2)	0.5029(2)	0.091(7)
C(33)	0.3413(3)	0.0552(2)	0.7463(2)	0.045(2)	H(25)	-0.2719(4)	0.0118(2)	0.5979(2)	0.091(7)
C(34)	0.4579(3)	0.0751(2)	0.7504(2)	0.043(2)	H(26)	-0.0680(4)	0.0358(2)	0.5976(2)	0.091(7)
C(35)	0.5126(3)	0.0971(2)	0.6929(2)	0.049(2)	H(32)	0.1994(3)	0.0435(2)	0.6819(2)	0.091(7)
C(36)	0.4508(3)	0.0992(2)	0.6313(2)	0.041(2)	H(33)	0.3038(3)	0.0401(2)	0.7858(2)	0.091(7)
C(41)	-0.0360(24)	0.2500(0)	0.2500(15)	0.069(8)	H(34)	0.5005(3)	0.0737(2)	0.7928(2)	0.091(7)
C(42)	-0.0111(13)	0.2016(6)	0.2404(7)	0.032(4)	H(35)	0.5928(3)	0.1109(2)	0.6957(2)	0.091(7)
C(43)	0.0932(19)	0.1995(8)	0.1936(10)	0.044(5)	H(36)	-0.0360(24)	0.2500(0)	0.2500(15)	0.069(8)
C(44)	0.1452(25)	0.2500(0)	0.1663(14)	0.066(8)					
C(41')	-0.0661(17)	0.2269(7)	0.2656(10)	0.078(7)					
C(42')	0.0338(15)	0.1969(7)	0.2207(9)	0.044(5)					
C(43')	0.1187(20)	0.2209(8)	0.1820(11)	0.072(8)					

Table 7. Structural data for adducts 3 and 6

	3 (at 296 K)	6 (at 193 K)
Cell dimensions		
a (Å)	9.903(2)	11.222(3)
b (Å)	11.332(4)	19.743(9)
c (Å)	12.739(3)	24.984(6)
α (°)	79.52(2)	90
β (°)	73.70(2)	90
γ (°)	70.48(3)	90
V (Å ³)	1286.9(9)	5537(3)
Space group	$P\bar{1}$	$Pnma$
Molecules per unit cell	1	4
Number of unique observed reflexions ($F/\sigma_F \geq 3$)	1625	1642
Scan range in 2Θ (°)	3–45	3–60
ω -scan data collection background: scantime ratio	1:1	1:1
Maximum rest electron density ($e/\text{Å}^3$)	0.21	0.35
R -values: R	0.064	0.086
R_w	0.052	0.093
g	$9 \cdot 10^{-5}$	$8.7 \cdot 10^{-4}$

$R = \Sigma(|F_o - F_c|)/\Sigma F_o$
 $R_w = \Sigma((|F_o - F_c|) \cdot w^{-2})/\Sigma(F_o \cdot w^{-2}), \quad w = 1/(\sigma^2(F_o) + g \cdot F_o^2)$

- 1) M. Yalpani, R. Köster, and G. Wilke, Chem. Ber. **116**, 1336 (1983).
- 2) W. L. Fielder, M. M. Chamberlain, and C. H. Brown, J. Org. Chem. **26**, 2154 (1961).
- 3) D. L. Yabroff and G. E. Branch, J. Am. Chem. Soc. **54**, 2569 (1932); **55**, 1663 (1933).
- 4) H. R. Snyder, M. S. Konecky, and W. J. Lennarz, J. Am. Chem. Soc. **80**, 3611 (1958).
- 5) R. Lutter, Ph. D. Thesis, Univ. Marburg 1979.
- 6) J. M. Ritchey, Ph. D. Thesis, University of Colorado 1968.
- 7) H. C. Brown and R. B. Johannesen, J. Am. Chem. Soc. **75**, 16 (1953).
- 8) C. Krüger and Y. H. Tsay, unpublished results.
- 9) P. H. Clippard, J. C. Hanson, and R. C. Taylor, J. Cryst. Mol. Struct. **1**, 363 (1971).
- 10) J. Schulze, R. Boese, and G. Schmid, Chem. Ber. **114**, 1297 (1981).
- 11) K. Anton, K. Fußstetter, and H. Nöth, Chem. Ber. **114**, 2723 (1981).
- 12) K. Anton and H. Nöth, Chem. Ber. **115**, 2668 (1982).
- 13) G. M. Sheldrick, SHELXTL (1981), an integrated system for solving, refining, and displaying crystal structures from diffraction data. University of Göttingen.

[35/83]